Gulf Journal of Mathematics
Vol 17, Issue 1 (2024) 110-129

ISSN: 2309-4966
https://doi.org/10.56947/gjom.v17i1.1980

STABILITY ANALYSIS OF GRAVITY MODULATED THERMOSOLUTAL CONVECTION IN CASSON FLUID WITH INTERNAL HEAT SOURCE

CHANDAN K.G.[1], AKHILA P.A.[2] and PATIL MALLIKARJUN B.[3*]

Abstract. The current work establishes research into the non-Newtonian Casson fluid's linear and weakly non-linear stability analysis under the influences of internal heating and gravitational modulation. The study is confined to stationary convection, where marginal stability is determined by the critical Rayleigh number, which is derived from linear stability analysis. The marginal stability curves are plotted to observe the onset of convection due to different parameters that exist in the problem. Heat and mass transfer are measured in terms of the Nusselt number (Nu) and Sherwood number (Sh), respectively, in the non-linear stability analysis. These measurements are based on the Ginzburg-Landau (GL) equation. One of the main outcomes of this stability analysis is that the internal Rayleigh number and Casson parameter behave similarly for mass transport in a fluid whereas it operates oppositely for heat transfer in a fluid.

1. Introduction and preliminaries

The Rayleigh-Bénard convection (RBC), which is the most often investigated convection phenomenon due to its analytical and experimental convenience, offers the foundation for double-diffusive convection. The criterion for the onset situation was established by Béniard [1], who independently came to the same conclusion from experiments as Thomson [2]. However, it was Rayleigh [3] who successfully put up a theoretical framework for it and discovered a nondimensional parameter termed as the Rayleigh number. One of the well-known non-Newtonian viscoplastic fluids is Casson fluid, which was initially presented in 1959 by Casson [4]. This fluid exhibits two different behaviours according to its yield stress. Based on the yield stress P_y, this exhibits both viscous fluid and rigid solid behaviour. This reveals pseudo-plastic behaviour as well, provided that the shear stress is moderately high.

The Bingham fluid and mathematical model was initially put forward by Bingham [5] around the turn of the 20th century. The most basic strategy for handling yield stress is the Bingham model. A different acronym for this fluid is Casson

Date: Received: May 6, 2024; Accepted: Jun 10, 2024.

* Corresponding author.

2020 *Mathematics Subject Classification.* 35Q35; 70K20.

Key words and phrases. Casson fluid, thermosolutal convection, Gravity modulation, heat and mass transfer, Internal heating.

fluid. Casson fluids are widely employed in the production of paint, synthetic lubricants, China clay products, pharmaceuticals, coal processing, and other industries. Moreover, Casson fluid is utilized to make jelly, tomato sauce, sewage sludge, biological fluids, and synovial fluids. These fluids also serve a purpose in the food processing industry, biological treatments, bioengineering, and drilling operations, among numerous additional uses. Scientists and researchers are focusing a great deal of their attention on Casson fluids with various impacts because of their broad variety of applications. Unsteady two-dimensional flow throughout a stretching surface for the Casson fluid was studied by Swathi *et al.*[6]. Casson fluid's boundary layer flow was studied by Pramanik [7] by considering heat transfer through an exponential stretching surface and this functions when there are blowing or suction effects at the surface. Under boundary layer theory, Imran *et al.*[8] examined the study of two-dimensional flow with a stretching wedge submerged in Casson fluid, producing a hydromagnetic effect. Heat transport and the suction/injection effect are used in this case and are investigated numerically. In [9] Rahman *et al.* examined the non-Newtonian Maxwell fluid flow with slip at the boundary. The unsteady flow of a Casson fluid in a porous medium with an infinite vertical oscillating plate embedded with an applied MHD was solved and obtained exact solutions by Abid *et al.*[10]. The thermal conductivity and temperature-dependent viscous term movement of a steady, incompressible Casson fluid flow were examined by Animasaun *et al.*[11]. In an exponentially stretching sheet, the magnetohydrodynamic effect is used to study natural convection. The study also takes into account the suction effect and internally generated heat generation that decays exponentially. A study on bi-viscous Bingham fluid using both linear and non-linear analysis was conducted by Keerthana *et al.*[12].

Regarding buoyancy-driven convection in hydromagnetic Casson fluid, Frigaard *et al.* [13] commented. A magnetic field had been added to the Casson fluid under the Soret and Dufour effect by Hayat *et al.*[14]. Raza *et al.*[15] identified several solutions for this same fluid by applying mixed convection under the influence of a magnetic field. Similar to this, Shehzad *et al.*[16] studied applied magnetohydrodynamics and the heating impact to this fluid in a porous media in three dimensions. To investigate the mixed convective flow of Casson fluid, Bilal *et al.*[17] takes into account the stretching sheet concept while taking convective boundary conditions and the Hall effect into consideration. Ganesh *et al.*[18] investigated the effects of double-diffusive convection and thermal radiation in Casson fluid using the same stretching sheet on a vertical surface. Next comes,The fluid's mass and heat transfer as a result of several effects. The Nusselt and Sherwood number values for Casson fluid were investigated by Parmar *et al.*[19]. The effects of Joule heating and viscous dissipation was studied by Medisetty *et al.*[20] for flow of two immiscible liquids in an inclined channel. Mukhopadhyay *et al.*[21] conducted a study on non-Newtonian Casson fluid flow over an unsteady stretching sheet. Mustafa *et al.*[22] introduced the boundary layer idea on the Casson fluid on the moving plate.

Comparably, other researchers [23]-[27] produced important work on Casson fluid flow. A study on Rayleigh Bénard convection (RBC) in non-Newtonian fluid was conducted by Turan *et al.*[23]. Additionally, a bifurcation between the

convection and conduction regimes was discovered and a supercritical transition was noted in a mathematical experiment carried out on the same by Aghighi *et al.*[24]. Aneja *et al.*[25] investigated the free convection of Casson fluid in a porous cavity with moderate heat and thus they concluded that as the Casson fluid parameter and the Darcy number increased, so did the flow circulation and heat-transfer rate. Unsteady double diffusive convection in Casson fluid saturating a porous media was examined by Das *et al.*[26]. Their research shows that the buoyancy force causes temperature gradients and concentration at the upper layer to rise along with an increase in mass and heat transport close to the plate. An analytical investigation on thermal RBC in a Casson fluid and hybrid nanofluid was conducted by Shruthy *et al.*[27]. They discovered that whereas an increased Casson parameter in a Casson fluid delays the commencement of convection and thereby increases heat transfer in the medium, in a hybrid nanofluid, convection occurs more slowly and heat transport is boosted.

Along with temperature and rotational modulation, gravity modulation has been the subject of much research in the last few decades. The effects of gravity modulation on the beginning of convection in both porous and fluid layers are examined in [28] and [29]. However, Chen and Chen [30] explored the stability of convection in a vertical channel and investigated the impact of gravity modulation. Additionally, Vanishree and Anjana [31] studied gravity modulation in Oldroyd-b liquids by introducing double diffusive convection. Siddheshwar *et al.*[32] did extremely important work on the linear, local non-linear, and weakly non-linear stability analysis of stationary double-diffusive convection in a dielectric liquid under the impact of gravity modulation. Double diffusive convection in a Newtonian liquid was studied by Bhadauria and Kiran [33] using the same gravity modulation and the introduction of magnetic effect. Additionally, young researcher Kiran [34] and [35] investigated oscillatory double-diffusive convection under the impact of gravity modulation in a viscoelastic fluid layer. They looked into a fluid layer experiencing weakly non-linear thermal convection and a similar effect.

In the present work, we primarily extended the work of Akhila *et al.*[36] by using Ginzberg Landau equation to study stationary convection in Casson fluid under gravity modulation and internal heating impact. The study of heat and mass transport in the Casson fluid versus different parameters—which are also graphically represented—follows from the amplitude equation that is thus generated. Because of the various time scales, each graphical output shows how various parameters affect the system's heat transfer rate. Additionally, the wavenumber that determines the onset of convection is displayed against the marginal stability curves for the critical Rayleigh number. The main improvement is displayed in visuals 3c and 4c, which demonstrate that mass transfer and heat production are inversely related to increasing values of internal Rayleigh numbers for similar values of Ri.

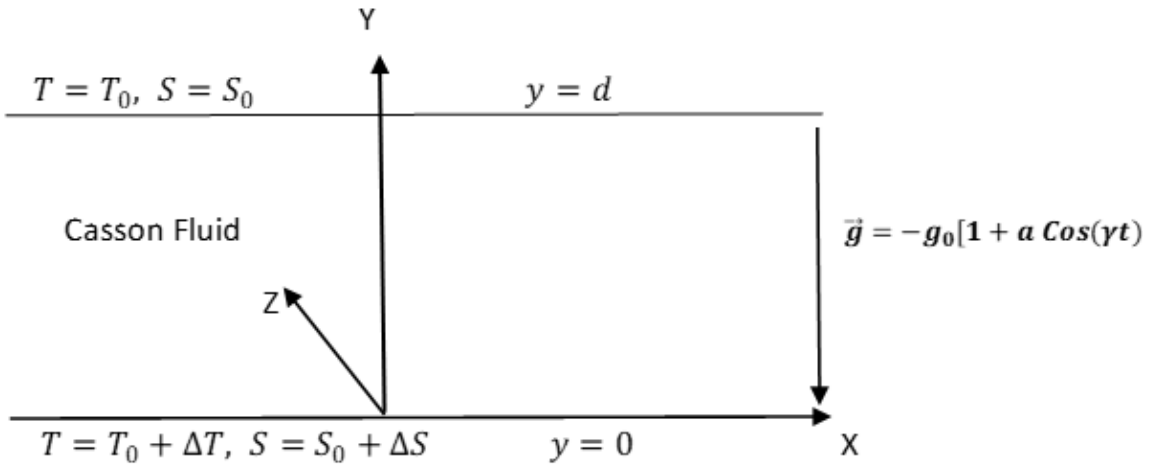


FIGURE 1. Physical Configuration for thermosolutal convective flow of Casson fluid.

2. Problem Statement and Formulation

In this growing study, a horizontal layer of Casson fluid comprising a fluid layer of thickness d is taken into consideration. The flow region is defined as $R = \{(x, y)/\ y \in [0, d], x \in [-\infty, \infty]\}$ and is limited to a two-dimensional domain. When Rayleigh-Benard Convection is taken into account, the lower end is heated or cooled; the upper and lower plates, with temperatures $T_0 + \Delta T$ and T_0, respectively, are squeezed between $y = 0$ and $y = d$. $S_0 + \Delta S$ and S_0, respectively, represent the solute concentrations at the bottom and upper plates. The gravitational force is operating in a vertical downward direction, and Figure 1 displays the entire physical structure.

The following are the governing equations for mass conservation, momentum conservation, energy conservation, and concentration conservation under the Oberbeck Boussinesq approximation [12, 36]:

$$\nabla \cdot \vec{q} = 0 \tag{2.1}$$

$$\rho_0 \frac{D\vec{q}}{Dt} = -\nabla p - \rho g_0[1 + a\ \cos(\gamma t)]\hat{j} + \nabla \cdot \mathcal{T} \tag{2.2}$$

$$\frac{DT}{Dt} = \kappa_T \nabla^2 T + Q(T - T_0) \tag{2.3}$$

$$\frac{DS}{Dt} = \kappa_S \nabla^2 S \tag{2.4}$$

$$\rho = \rho_0(1 - \alpha^*) \tag{2.5}$$

The stress tensor $\mathcal{T}$ in the Casson fluid rheological model is symbolized as [7]:

$$\tau_{ij} = 2\begin{cases}(\mu_B + \frac{Py}{\sqrt{2\Pi}})e_{ij} & \Pi > \Pi_c \\ (\mu_B + \frac{Py}{\sqrt{2\Pi}})e_{ij} & \Pi < \Pi_c\end{cases} \tag{2.6}$$

where $e_{ij} = \frac{1}{2}\left(\frac{\partial q_i}{\partial x_j} + \frac{\partial q_j}{\partial x_i}\right)$, $\alpha^* = \alpha_1(T - T_0) + \alpha_2(S - S_0)$ and μ_B is dynamic viscosity. One example of a non-Newtonian fluid is the Casson fluid, whose yield stress, represented by P_y, is a non-Newtonian fluid (NNF) whose threshold value of the rate of deformation is shown by Π_c.
On substituting the above equation in Eq.(2.2), we get

$$\rho_0\frac{D\vec{q}}{Dt} = -\nabla p - \rho g_0[a\,\cos(\gamma t) + 1]\hat{j} + \mu_B\nabla\cdot\left[\left(1 + \frac{P_y}{\mu_B\sqrt{2\Pi}}\right)\left(\nabla\vec{q} + \nabla\vec{q}^T\right)\right] \tag{2.7}$$

Basic State

Upon the fluid at rest, we possess

$$T = T_b(y), \quad S = S_b(y), \quad p = p_b(y), \quad \rho = \rho_b(y), \quad \vec{q} = \vec{q_b} = (0, 0) \tag{2.8}$$

On substituting the above equation into Eqs.(2.3 - 2.5) and (2.7) we obtain,

$$\frac{dp_b}{dy} + \rho_b(y)g_0 = 0 \tag{2.9}$$

$$\frac{d^2T_b}{dy^2} + \frac{Q}{\kappa_T}T_b = \frac{Q}{\kappa_T}T_0 \tag{2.10}$$

$$\frac{d^2S_b}{dy^2} = 0 \tag{2.11}$$

$$\rho_b = \rho_0(1 - \alpha^{**}) \tag{2.12}$$

Where $\alpha^{**} = \alpha_1(T_b(y) - T_0) + \alpha_2(S_b(y) - S_0)$. Equations (2.10) and (2.11) can be solved using the boundary conditions $T_b = T_0 + \Delta T$, $S_b = S_0 + \Delta S$ and $T_b = T_0$, $S_b = S_0$ at $y = 0$ and $y = d$ respectively, we get

$$T_b(y) = \left(\frac{\mathrm{Sin}\sqrt{R_i}(1 - \frac{y}{d})}{\mathrm{Sin}\sqrt{R_i}}\right)\Delta T + T_0 \tag{2.13}$$

$$S_b(y) = \left(1 - \frac{y}{d}\right)\Delta S + S_0 \tag{2.14}$$

Perturbed State

By superimposing the perturbations on the basic state solution, the following perturbed equations are produced.

$$p = p_b(y) + p', \quad \vec{q} = \vec{q_b} + \vec{q'}, \quad \rho = \rho_b(y) + \rho', \quad T = T_b(y) + T', \quad S = S_b(y) + S' \tag{2.15}$$

where the prime denotes the perturbed quantities. On introducing the above equation into Eqs. (2.1), (2.3 -2.5) and (2.7), we obtain

$$\nabla \cdot \vec{q}^{'} = 0 \tag{2.16}$$

$$\rho_0 \frac{D\vec{q}^{'}}{Dt} = -\nabla p^{'} + \left(\frac{1}{\beta} + 1\right) \mu_B \nabla^2 \vec{q}^{'} - \rho^{'} g_0 [a\, \cos(\gamma t) + 1]\hat{j} \tag{2.17}$$

$$\frac{D\vec{T}^{'}}{Dt} + v^{'} \left(\frac{\partial T_b}{\partial y}\right) = \kappa_T \nabla^2 T^{'} + Q(T^{'}) \tag{2.18}$$

$$\frac{D\vec{S}^{'}}{Dt} + v^{'} \left(\frac{\partial S_b}{\partial y}\right) = \kappa_S \nabla^2 S^{'} \tag{2.19}$$

$$\rho^{'} = -\rho_0 \alpha_1 T^{'} + \rho_0 \alpha_2 S^{'} \tag{2.20}$$

The Casson fluid parameter can be obtained by

$$\beta = \frac{\mu_B \sqrt{2\Pi}}{P_y} \tag{2.21}$$

The pressure term is omitted and the stream function ψ is inserted as follows:

$$u^{'} = \frac{\partial \psi}{\partial y}, \quad v^{'} = -\frac{\partial \psi}{\partial x} \tag{2.22}$$

The governing equations take the following form after the primes are eliminated:

$$\rho_0 \frac{\partial}{\partial t}(\nabla^2 \psi) = -\rho_0 \alpha_1 g_0 \left[1 + a\, \cos(\gamma t)\right] \frac{\partial T^{'}}{\partial x} + \rho_0 \alpha_2 g_0 \left[1 + a\, \cos(\gamma t)\right] \frac{\partial S^{'}}{\partial x} + \mu_B \left(1 + \frac{1}{\beta}\right) \nabla^4 \psi + \rho_0 J(\psi, \nabla^2 \psi) \tag{2.23}$$

$$\left(\frac{\partial}{\partial t} - \kappa_T \nabla^2 - Q\right) T^{'} = \frac{\partial \psi}{\partial x} \frac{\partial T_b}{\partial y} + J(\psi, T^{'}) \tag{2.24}$$

$$\left(\frac{\partial}{\partial t} - \kappa_S \nabla^2\right) S^{'} = -\frac{\partial \psi}{\partial x} \frac{\Delta S^{'}}{d} + J(\psi, S^{'}) \tag{2.25}$$

The definitions presented below allow us to non-dimensionalize Eqs. (2.23 - 2.25) as

$$t^* = \frac{t\kappa_T}{d^2}, \quad (x^*, y^*) = \left(\frac{x}{d}, \frac{y}{d}\right), \quad \theta^* = \frac{T}{\Delta T}, \quad S^* = \frac{S}{\Delta S}, \quad \psi^* = \frac{\psi}{\kappa_T}, \quad \Omega = \frac{\gamma d^2}{\kappa_T} \tag{2.26}$$

After deleting the asterisks from the non-dimensionalized form of Eqs. (2.23 - 2.25), we attain

$$\frac{1}{Pr} \frac{\partial}{\partial t} \nabla^2 \psi = \frac{1}{Pr} J(\psi, \nabla^2 \psi) + [1 + a\cos(\Omega t)] \left(Ra_S \frac{\partial S}{\partial x} - Ra_T \frac{\partial \theta}{\partial x}\right) + \left(1 + \frac{1}{\beta}\right) \nabla^4 \psi \tag{2.27}$$

$$\frac{\partial \psi}{\partial x} + \left(\frac{\partial}{\partial t} - \nabla^2 - R_i\right) \theta = J(\psi, \theta) \tag{2.28}$$

$$\frac{\partial \psi}{\partial x} + \left(\frac{\partial}{\partial t} - \frac{1}{Le} \nabla^2\right) S = J(\psi, S) \tag{2.29}$$

where $Ra_T = \frac{\rho_0 \alpha_1 d^3 \Delta T g_0}{\kappa_T \mu_B}$, $Pr = \frac{\mu_B}{\rho_0 \kappa_T}$, $Ra_S = \frac{\rho_0 \alpha_2 d^3 \Delta S g_0}{\kappa_T \mu_B}$, $Le = \frac{\kappa_T}{\kappa_S}$. The boundary condition with regard to y, which is horizontal, isothermal, and stress-free, is applied while solving Eqs.(2.27 - 2.29):

$$\psi = \theta = S = \frac{\partial^2}{\partial y^2}\left(\frac{\partial \psi}{\partial x}\right) = 0 \quad \text{at} \quad y = 0, 1 \tag{2.30}$$

3. Linear Stability Analysis

We have now arrived at the prerequisite for the onset of convection. Using the boundary conditions (2.30) in Eqs. (2.27 - 2.29), we remove the non-linear terms like Jacobian. It is presumed that the following are the solutions:

$$\psi = A\ \mathrm{g}(y)\ \sin(k_c x) \tag{3.1}$$
$$\theta = B\ \mathrm{g}(y)\ \cos(k_c x) \tag{3.2}$$
$$S = C\ \mathrm{g}(y)\ \cos(k_c x) \tag{3.3}$$

where, $\mathrm{g}(y) = \sin(\pi y)$. A, B and C are stream function, temperature, and concentration of Casson fluid respectively, are all extremely tiny amplitudes. Substituting above equations in Eqs.(2.27 - 2.29), we get the critical Rayleigh number for the stationary mode of convection:

$$R_{a_c} = (\delta^2 - R_i)\left[\frac{Ra_S Le}{\delta^2} + \left(1 + \frac{1}{\beta}\right)\frac{\delta^4}{k_c^2}\right] \tag{3.4}$$

where, k_c is the wavenumber for convecting cell at onset and $\delta^2 = k_c^2 + \pi^2$.

4. Non-Linear Instability

In non-linear analysis, we examine the mass transport rate and heat transport. Since the oscillations are thought to be quite little, we use $a = \epsilon^2 \delta_2$ where ϵ is a tiny quantity. It is also assumed that the time scale is $\tau = \epsilon^2 t$. Below are the asymptotic expansions in Ra_T, ψ, θ and S:

$$Ra_T = R_a + \epsilon^2 R_2 + \epsilon^4 R_4 + ..., \tag{4.1}$$
$$\psi = \epsilon\psi_1 + \epsilon^2\psi_2 + \epsilon^3\psi_3 + ..., \tag{4.2}$$
$$\theta = \epsilon\theta_1 + \epsilon^2\theta_2 + \epsilon^3\theta_3 + ..., \tag{4.3}$$
$$S = \epsilon S_1 + \epsilon^2 S_2 + \epsilon^3 S_3 + ..., \tag{4.4}$$

Above equations yield the ψ, θ and S values that meet the boundary constraints specified in Eq. (2.30). By incorporating the values from above equations in Eqs. (2.27-2.29), which yields the lowest order matrix given by:

$$\begin{bmatrix} -\left(\frac{1}{\beta}+1\right)\nabla^4 & -R_a\frac{\partial}{\partial x} & R_S\frac{\partial}{\partial x} \\ \frac{\partial}{\partial x} & -(\nabla^2 + R_i) & 0 \\ \frac{\partial}{\partial x} & 0 & -\frac{1}{Le}\nabla^2 \end{bmatrix} \begin{bmatrix} \psi_1 \\ \theta_1 \\ S_1 \end{bmatrix} = \begin{bmatrix} 0 \\ 0 \\ 0 \end{bmatrix} \tag{4.5}$$

Subject to the boundary constraints in Eq. (2.30), the first-order solution is provided as follows.

$$\psi_1 = A(\tau)\ \mathrm{g}(y)\ \sin(k_c x) \tag{4.6}$$

$$\theta_1 = \frac{-k_c}{\delta^2 - R_i} A(\tau)\ \mathrm{g}(y)\ \cos(k_c x) \tag{4.7}$$

$$S_1 = \frac{-k_c Le}{\delta^2} A(\tau)\ \mathrm{g}(y)\ \cos(k_c x) \tag{4.8}$$

5. Heat and Mass Transfer and Amplitude-Equation

The matrix of second order is provided by

$$\begin{bmatrix} -\left(\frac{1}{\beta}+1\right)\nabla^4 & -R_a\frac{\partial}{\partial x} & R_S\frac{\partial}{\partial x} \\ \frac{\partial}{\partial x} & -(R_i+\nabla^2) & 0 \\ \frac{\partial}{\partial x} & 0 & -\frac{1}{Le}\nabla^2 \end{bmatrix} \begin{bmatrix} \psi_2 \\ \theta_2 \\ S_2 \end{bmatrix} = \begin{bmatrix} R_{21} \\ R_{22} \\ R_{23} \end{bmatrix} \tag{5.1}$$

where,

$$R_{21} = 0 \tag{5.2}$$

$$R_{22} = \frac{-k_c^2\pi}{2(\delta^2 - R_i)} A(\tau)^2 \sin(2\pi y) \tag{5.3}$$

$$R_{23} = \frac{-k_c^2\pi Le}{2(\delta^2)} A(\tau)^2 \sin(2\pi y) \tag{5.4}$$

By considering attention to the boundary conditions in Eq. (2.30), the second order solutions are as follows:

$$\psi_2 = 0 \tag{5.5}$$

$$\theta_2 = \frac{-k_c^2\pi}{2(\delta^2 - R_i)(4\pi^2 - R_i)} A(\tau)^2 \sin(2\pi y) \tag{5.6}$$

$$S_2 = \frac{-k_c^2 Le^2}{8\delta^2\pi} A(\tau)^2 \sin(2\pi y) \tag{5.7}$$

The subsequent are corresponding expressions for heat and mass transmission (Nu and Sh):

$$Nu = 1 + \frac{k_c^2\pi^2 \mathrm{Sin}\sqrt{R_i}}{(\delta^2 - R_i)(4\pi^2 - R_i)\sqrt{R_i}\mathrm{Cos}\sqrt{R_i}} A(\tau)^2 \tag{5.8}$$

$$Sh = 1 + \frac{k_c^2 Le}{4\delta^2} A(\tau)^2 \tag{5.9}$$

The matrix of third-order is supplied by

$$\begin{bmatrix} -\left(\frac{1}{\beta}+1\right)\nabla^4 & -R_a\frac{\partial}{\partial x} & R_S\frac{\partial}{\partial x} \\ \frac{\partial}{\partial x} & -(\nabla^2+R_i) & 0 \\ \frac{\partial}{\partial x} & 0 & -\frac{1}{Le}\nabla^2 \end{bmatrix} \begin{bmatrix} \psi_3 \\ \theta_3 \\ S_3 \end{bmatrix} = \begin{bmatrix} R_{31} \\ R_{32} \\ R_{33} \end{bmatrix} \tag{5.10}$$

ψ_3, θ_3 and S_3 meet the boundary requirements stated in (2.30). Upon switching ψ_1, S_1, θ_1, θ_2 and S_2 from Eqs. (4.6-4.8) and Eqs.(5.6-5.7), we obtain

$$\begin{aligned} R_{31} &= -\frac{k_c^2 A}{\delta^2 - R_i} R_a \left(\frac{R_2}{R_a} + \delta_2 \cos(\Omega\tau)\right) \sin(k_c x) \mathrm{g}(y) \\ &\quad -\frac{k_c^2 LeA}{\delta^2} Ra_S \delta_2 \cos(\Omega\tau) \sin(k_c x) \mathrm{g}(y) \\ &\quad +\frac{\delta^2 A_\tau}{Pr} \sin(k_c x) \mathrm{g}(y) \end{aligned} \tag{5.11}$$

$$\begin{aligned} R_{32} &= -\frac{k_c^3 A^3 \pi^2}{2(\delta^2 - R_i)(4\pi^2 - R_i)} \cos(k_c x) \left[\sin(3\pi y) - \mathrm{g}(y)\right] \\ &\quad +\frac{k_c A_\tau}{\delta^2 - R_i} \cos(k_c x) \mathrm{g}(y) \end{aligned} \tag{5.12}$$

$$\begin{aligned} R_{33} &= -\frac{Le^2 k_c^3 A^3}{8\delta^2} \cos(k_c x) \left[\sin(3\pi y) - \mathrm{g}(y)\right] \\ &\quad +\frac{k_c LeA_\tau}{\delta^2} \cos(k_c x) \mathrm{g}(y) \end{aligned} \tag{5.13}$$

The third-order solution is required to satisfy the following solvability requirement:

$$\int_{y=0}^{y=1} \int_{x=0}^{x=\frac{2\pi}{k_c}} \left[\psi_1^* R_{31} + \theta_1^* R_{32} + S_1^* R_{33}\right] dxdy = 0 \tag{5.14}$$

where, ψ_1^*, θ_1^* and S_1^* are found by obtaining the adjoint of Eq.(4.5) and are given by

$$\psi_1^* = A(\tau)\ \sin(k_c x)\ \mathrm{g}(y) \tag{5.15}$$

$$\theta_1^* = \frac{-R_a k_c}{\delta^2 - R_i} A(\tau)\ \cos(k_c x)\ \mathrm{g}(y) \tag{5.16}$$

$$S_1^* = \frac{Ra_S k_c Le}{\delta^2} A(\tau)\ \cos(k_c x)\ \mathrm{g}(y) \tag{5.17}$$

Below is a depiction of the non-autonomous Ginzburg-Landau equation,

$$B_1 A_\tau + B_3 (A(\tau))^3 = B_2 A(\tau) \tag{5.18}$$

where,

$$B_1 = \frac{\delta^2}{Pr} + \frac{R_a k_c^2}{(\delta^2 - R_i)} - \frac{Ra_S K_c^2 Le}{\delta^4}$$

$$B_3 = \frac{R_a k_c^4 \pi^2}{2(\delta^2 - Ri)^2 (4\pi^2 - R_i)} - \frac{Ra_S k_c^4 Le^2}{8\delta^4}$$

$$B_2 = \frac{k_c^2}{\delta^2 - R_i} R_a \left(\frac{R_2}{R_a} + \delta_2 \cos(\Omega\tau)\right) - \frac{Ra_S Le k_c^2 \delta_2 \cos(\Omega\tau)}{\delta^2}$$

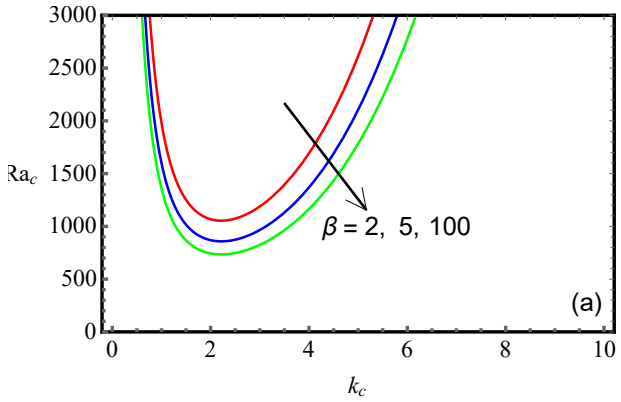


FIGURE 2a. k_c against R_{a_c} for various values of β.

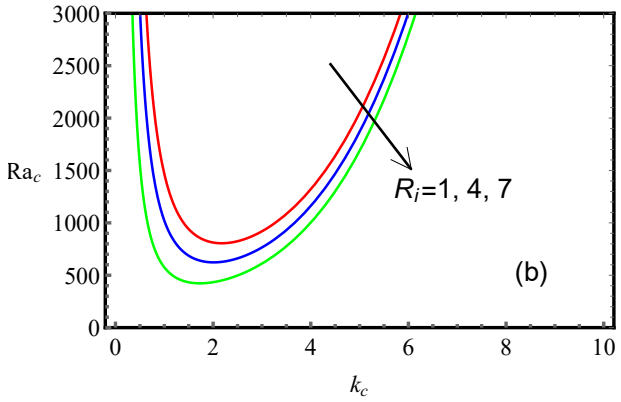


FIGURE 2b. k_c against R_{a_c} for various values of R_i.

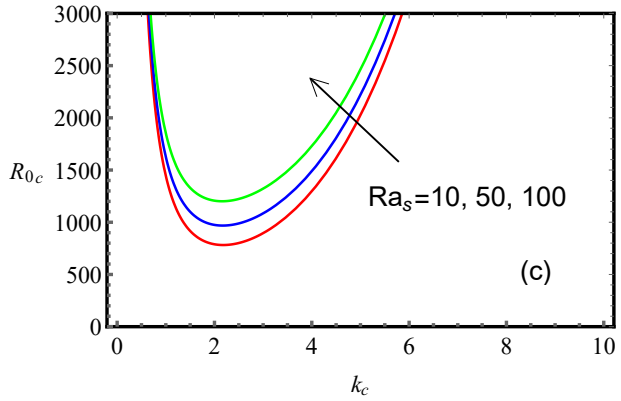


FIGURE 2c. k_c against R_{a_c} for various values of Ra_s.

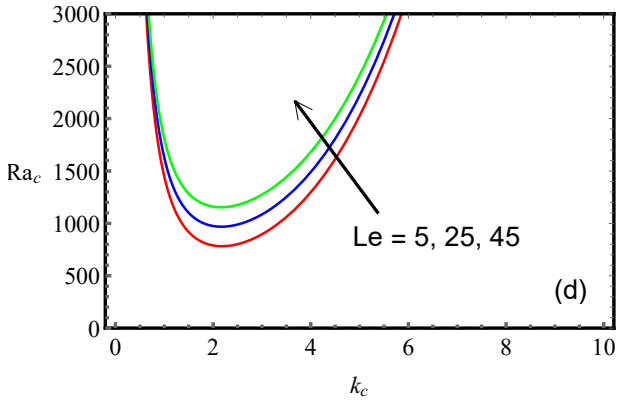


FIGURE 2d. k_c against R_{a_c} for various values of Le.

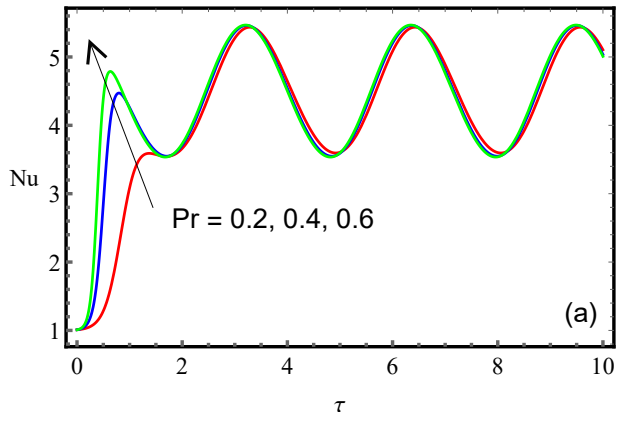


FIGURE 3a. τ against Nu for various values of Pr.

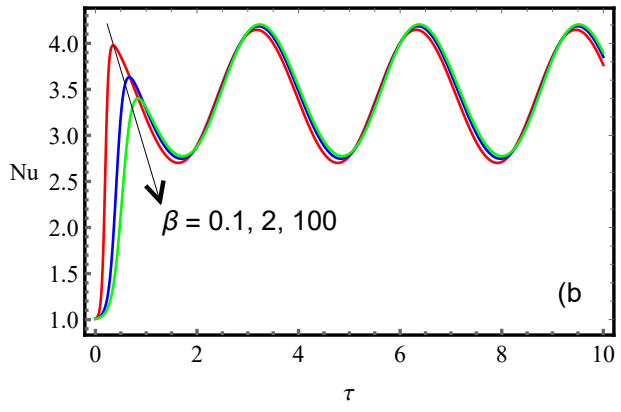


FIGURE 3b. τ against Nu for various values of β.

6. Results and Discussion

The study considered non-Newtonian Casson fluid and explores the weak nonlinear stationary convection under the internal heating effect and gravity modulation. The third-order finite amplitude equation of convection is found using

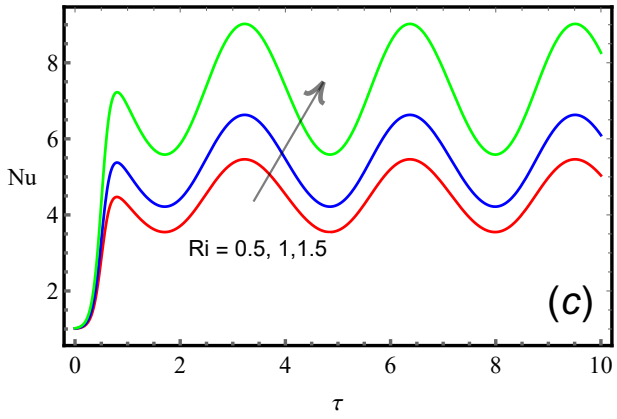


FIGURE 3*c*. τ against Nu for various values of Ri.

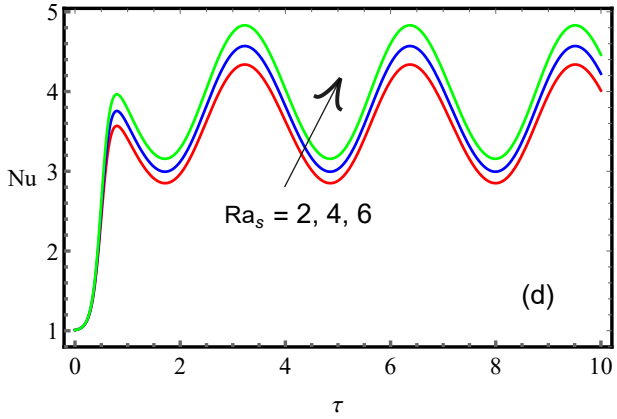


FIGURE 3*d*. τ against Nu for various values of Ra_s.

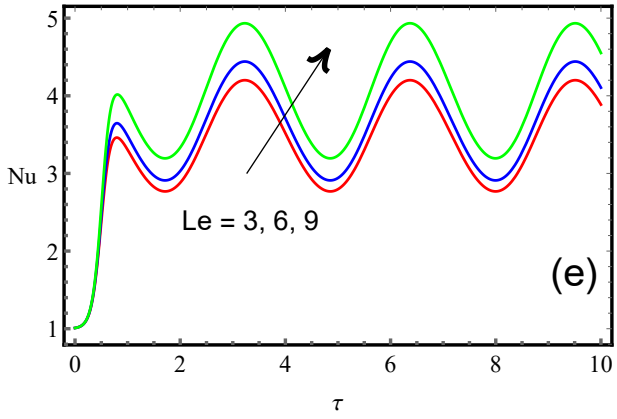


FIGURE 3*e*. τ against Nu for various values of Le.

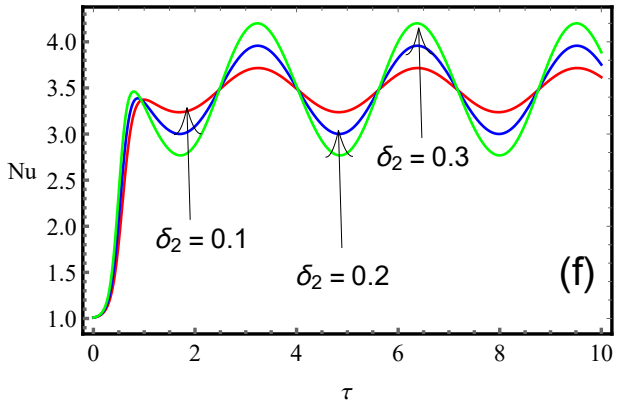


FIGURE 3f. τ against Nu for various values of δ_2.

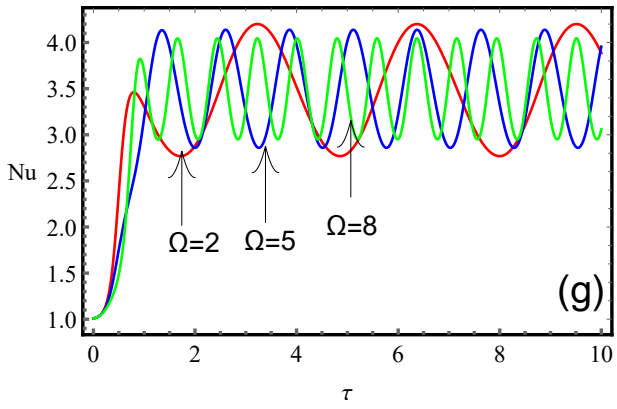


FIGURE 3g. τ against Nu for various values of ω.

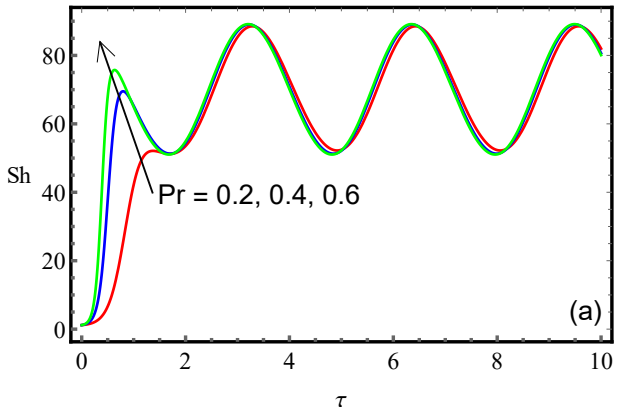


FIGURE 4a. τ against Sh for various values of Pr.

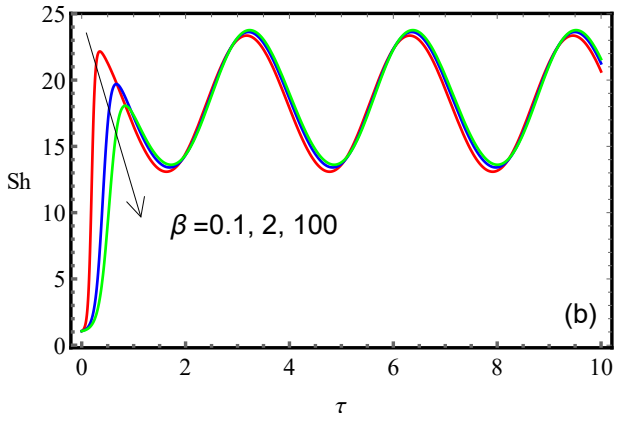


FIGURE 4*b*. τ against Sh for various values of β.

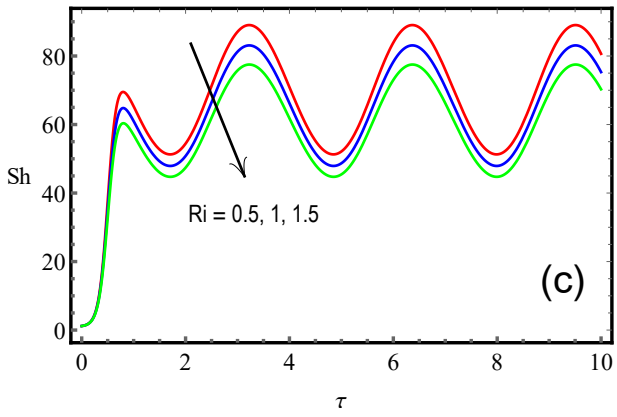


FIGURE 4*c*. τ against Sh for various values of R_i.

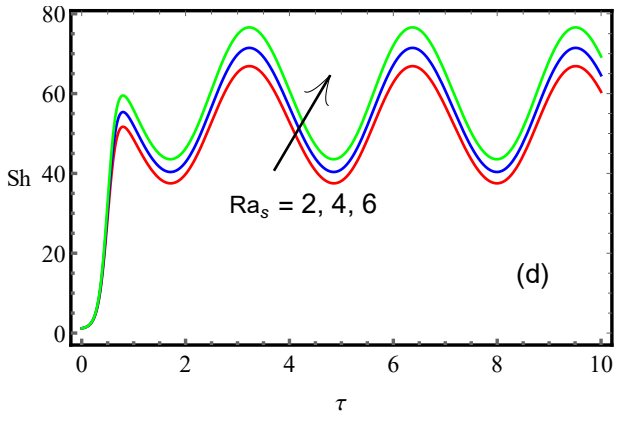


FIGURE 4*d*. τ against Sh for various values of Ra_s.

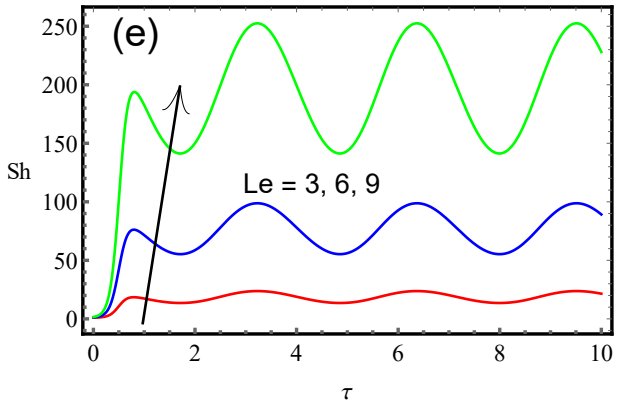


FIGURE 4e. τ against Sh for various values of Le.

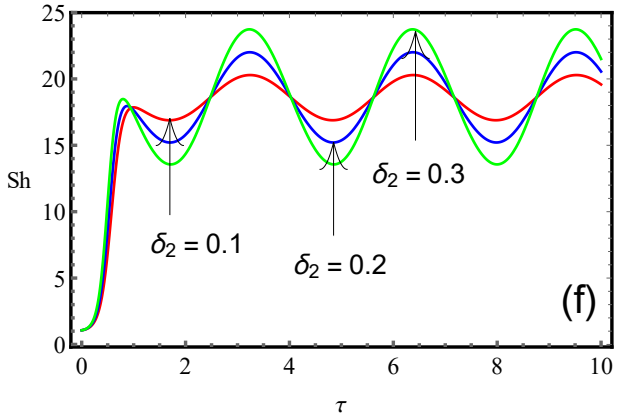


FIGURE 4f. τ against Sh for various values of δ_2.

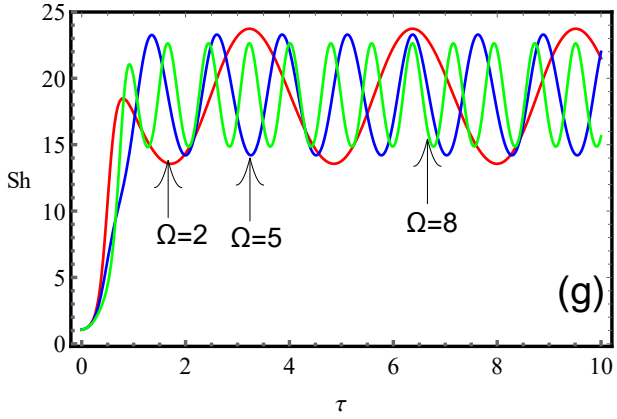


FIGURE 4g. τ against Sh for various values of ω.

the GLE model. To calculate the convection amplitude, the problem's gravity modulation is taken into account at $O(\epsilon^2)$ order. It is a well-known fact that stability analysis is derived from linear theory, whereas mass and heat transfer are assessed using nonlinear theory. Internal heating effect and gravity modulation govern the study of thermal instability in the Casson fluid layer, typically stated. This research examines heat and mass transmission in the Casson fluid layer using gravity modulation and the internal heating effect. The values of Pr, Ra_s, β, R_i, Le, δ_2, Ω, and other parameters are obtained approximately at their minimal values. It is clear from the relationship between β and P_y that lower values of β result in larger yield stress with decreased fluid flow. On the other hand, larger values of β result in less yield stress and increased fluid flow. The marginal stability of the system as a function of several parameters is shown in graphs in Fig.2. The impact of the Casson parameter β on the critical Rayleigh number is explained in Fig. 2(a). The onset of convection advances as the value of β grows, as indicated by a drop in the critical Rayleigh number. An analogous finding can be made for the internal Rayleigh number. As shown in Fig. 2(b), an increase in R_i causes the advancement in onset of convection. Nevertheless, the solutal Rayleigh number and Lewis number exhibit the opposite behavior. That is, an increase in the critical Rayleigh number indicates a delay in the onset of convection as the values of Ra_s and Le rise. One can look at these observations in Figs. 2(c) and 2(d).

The system's heat transport as a function of several parameters is shown in the following series of graphs. The value of the Nusselt number increases in tandem with the Prandtl number's value. This indicates that there is an increase in heat transport, as seen in Fig. 3(a). The impact of the Casson parameter on the system's heat transport is seen in Fig. 3(b). Initially, a decrease in heat transmission is noted when the value of β increases. The impacts of internal Rayleigh number, solutal Rayleigh number, and Lewis number are described in Figs. 3(c), 3(d), and 3(e). The Nusselt numbers grow together with the values of these parameters. Figs. 3(f) and 3(g) show the fluctuations in modulation frequency and amplitude.

The Sherwood number is shown against the time scale in the following collection of graphs. The graphs of mass transfer in the system caused by the Casson parameter and the Prandtl number, respectively, are shown in Figs. 4(a) and 4(b), where an opposite behaviour is seen. In other words, as the Prandtl number increases, mass transfer increases, and as the β number increases, mass transfer decreases in the system. Figs. 4(c) and 4(d), which are caused by internal Rayleigh number R_i and solutal Rayleigh number Ra_s, respectively, show a similar kind of observation.

Lewis number in mass transfer causes a significant shift in the modulation curve, as shown in Fig. 4(e). The amplitude of the mass transfer curves in the system changes dramatically with an increase in Lewis number. The mass transfer amplitude and frequency curves are shown in Figs. 4(f) and 4(g).

Conclusions

An examination is conducted into how internal heating affects the movement of a non-Newtonian Casson fluid. By perturbing the fluid, the linear and non-linear stability analysis for stationary convection is carried out. As convection advances, it is observed that the system becomes destabilized due to the Casson parameter and internal Rayleigh number, whereas the Lewis number and solutal Rayleigh number stabilize the system by delaying the onset of convection. Heat transport in the system is enhanced by the Prandtl, internal, solutal, and Lewis numbers; however, it declines by the Casson parameter β. The mass transfer of the system gets improved by the Lewis, Prandtl, and solutal Rayleigh numbers. On the other hand, the internal Rayleigh number and the Casson parameter decrease mass transmission.

Nomenclature

Latin Symbols

A Streamline perturbation amplitude
Pr Prandtl number, $Pr = \dfrac{\mu_B}{\rho_0 \kappa_T}$
d Dimensional layer depth
κ_T Thermal Diffusivity of the medium
κ_S species diffusivity
Le Lewis number, $Le = \dfrac{\chi}{\kappa_S}$
p Pressure
$\vec{g}$ Acceleration due to gravity
Ra_T Thermal Rayleigh number
Ra_S Solutal Rayleigh number
R_{a_c} Critical Rayleigh number
τ Time
T Temperature
Nu Nusselt number
Sh Sherwood number
$\frac{D}{Dt}$ The material derivative.
S Solute concentration
ΔT Difference in temperature
(x^*, y^*, z^*) Cartesian coordinates

Greek symbols

ϵ Perturbation parmeter
Ω Modulation frequency
α_1 Thermal expansion coefficient
α_2 Coefficient of solute expansion
δ^2 Horizontal wave number $k_c^2 + \pi^2$
β Casson fluid parameter
δ_2 Amplitude of gravity modulation
$\mathcal{T}$ Stress tensor of Casson fluid

P_y Yield Stress
Π Rate of deformation of Casson fluid
μ_B Dynamic viscosity
ρ Density of Casson fluid
τ Slow time scale $\tau = \epsilon^2 t$
ψ Stream function
ψ^* Dimensionless stream function
θ^* Dimensionless temperature

Subscripts

b Solution of basic state

Superscripts

$*$ Dimensionless variable
$'$ Perturbated variable

Conflict of interest

The authors state that there is no conflict of interest.

Acknowledgements

One of the authors Akhila P A would like to thank the financial assistance received from Karnataka Science and Technology Promotion Society (KSTePS) under the program of Karnataka DST - Ph.D fellowship for Science and Engineering: MAT- 03:2022-23/1019.

References

1. Bénard,H. (1901). Les tourbillons cellulaires dans une nappe liquide.-Méthodes optiques d'observation et d'enregistrement. Journal de Physique Théorique et Appliquée, 10(1), 254-266. https://doi.org/10.1051/jphystap:0190100100025400
2. Thomson, J. (1882). On a changing tesselated structure in certain liquids. Proc. Phil. Soc. Glasgow, 13, 464-468.
3. Rayleigh, L. (1916). LIX. On convection currents in a horizontal layer of fluid, when the higher temperature is on the under side. The London, Edinburgh, and Dublin Philosophical Magazine and Journal of Science, 32(192), 529-546. https://doi.org/10.1080/14786441608635602
4. Casson, N. (1959). Flow equation for pigment-oil suspensions of the printing ink-type. Rheology of disperse systems, 84-104.
5. Bingham, E. C. (1922). Fluidity and Plasticity. McCraw-Hill Book Company. Inc., New York, London, 439. https://doi.org/10.1007/BF02392308
6. Mukhopadhyay, S., De, P. R., Bhattacharyya, K., and Layek, G. C. (2013). Casson fluid flow over an unsteady stretching surface. Ain Shams Engineering Journal, 4(4), 933-938. https://doi.org/10.1016/j.asej.2013.04.004
7. Pramanik, S. (2014). Casson fluid flow and heat transfer past an exponentially porous stretching surface in presence of thermal radiation. Ain shams engineering journal, 5(1), 205-212. https://doi.org/10.1016/j.asej.2013.05.003
8. Ullah, I., Shafie, S., and Khan, I. (2017). MHD heat transfer flow of Casson fluid past a stretching wedge subject to suction and injection. Malaysian Journal of Fundamental and Applied Sciences, 13(4), 637-641. https://doi.org/10.11113/MJFAS.V13N4.745

9. Rahaman, K., Sankar, A., and Wolfe, E. (2024). Induced upper-convected Maxwell fluid flow in a cylinder oscillating longitudinally and torsionally with slip at the boundary. Gulf Journal of Mathematics, 16(2), 254-265. https://doi.org/10.56947/gjom.v16i2.1855
10. Hussanan, A., Salleh, M. Z., Khan, I., and Tahar, R. M. (2017). Heat transfer in magneto-hydrodynamic flow of a Casson fluid with porous medium and Newtonian heating. Journal of nanofluids, 6(4), 784-793. https://doi.org/10.1166/jon.2017.1359
11. Animasaun, I. L., Adebile, E. A., and Fagbade, A. I. (2016). Casson fluid flow with variable thermo-physical property along exponentially stretching sheet with suction and exponentially decaying internal heat generation using the homotopy analysis method. Journal of the Nigerian Mathematical Society, 35(1), 1-17. https://doi.org/10.1016/j.jnnms.2015.02.001
12. Keerthana, S., Siddheshwar, P. G., Tarannum, S., and Idris, R. (2023). Rayleigh–Bénard Convection in a Bi-viscous Bingham Fluid with Weak Vertical Harmonic Oscillations: Linear and Non-linear Analyses. International Journal of Applied and Computational Mathematics, 9(3), 30. https://doi.org/10.1007/s40819-023-01495-6
13. Frigaard, I. A., and Poole, R. J. (2021). Comment on "Bejan's flow visualization of buoyancy-driven flow of a hydromagnetic Casson fluid from an isothermal wavy surface"[Phys. Fluids 33 (9), 093113 (2021)]. Physics of Fluids, 33(12). https://doi.org/10.1063/5.0075898.
14. Hayat, T., Shehzad, S. A., and Alsaedi, A. (2012). Soret and Dufour effects on magnetohydrodynamic (MHD) flow of Casson fluid. Applied Mathematics and Mechanics, 33, 1301-1312. https://doi.org/10.1007/s10483-012-1623-6
15. Raza, J., Rohni, A. M., and Omar, Z. (2016). Multiple solutions of mixed convective MHD Casson fluid flow in a channel. Journal of Applied Mathematics, 2016. https://doi.org/10.1155/2016/7535793
16. Shehzad, S. A., Hayat, T., and Alsaedi, A. (2015). Three-dimensional MHD flow of Casson fluid in porous medium with heat generation. Journal of Applied Fluid Mechanics, 9(1), 215-223. https://doi.org/10.18869/acadpub.jafm.68.224.24042
17. Bilal Ashraf, M., Hayat, T., and Alsaedi, A. (2017). Mixed convection flow of Casson fluid over a stretching sheet with convective boundary conditions and Hall effect. Boundary Value Problems, 2017, 1-17. https://doi.org/10.1186/s13661-017-0869-7
18. Kumar, K. G., Ramesh, G. K., and Gireesha, B. J. (2016). Impact of thermal radiation on double-diffusive convection flow of Casson fluid over a stretching vertical surface. Front. Heat Mass Transf., 5, 1-8.
19. Parmar, A., and Jain, S. (2018). Exploration of heat and mass transfer in the convective slip flow of non-Newtonian Casson fluid. International Journal of Applied and Computational Mathematics, 4, 1-13. https://doi.org/10.1007/s40819-018-0498-6
20. Medisetty, P. D., Goyal, K., Suripeddi, S., and Badeti, S. (2024). Effects of different nanoparticles on the flow of two immiscible liquids in an inclined channel with Joule heating and viscous dissipation. Gulf Journal of Mathematics, 16(2), 278-290. https://doi.org/10.56947/gjom.v16i2.1815
21. Mukhopadhyay, S., De, P. R., Bhattacharyya, K., and Layek, G. C. (2013). Casson fluid flow over an unsteady stretching surface. Ain Shams Engineering Journal, 4(4), 933-938. https://doi.org/10.1016/j.asej.2013.04.004
22. Mustafa, M., Hayat, T., Pop, I., and Aziz, A. (2011). Unsteady boundary layer flow of a Casson fluid due to an impulsively started moving flat plate. Heat Transfer—Asian Research, 40(6), 563-576. https://doi.org/10.1002/htj.20358
23. Turan, O., Chakraborty, N., and Poole, R. J. (2010). Laminar natural convection of Bingham fluids in a square enclosure with differentially heated side walls. Journal of Non-Newtonian Fluid Mechanics, 165(15-16), 901-913. https://doi.org/10.1016/j.jnnfm.2010.04.013

24. Aghighi, M. S., Ammar, A., Metivier, C., and Gharagozlu, M. (2018). Rayleigh-Bénard convection of Casson fluids. International Journal of Thermal Sciences, 127, 79-90. https://doi.org/10.1016/j.ijthermalsci.2018.01.016
25. Aneja, M., Chandra, A., and Sharma, S. (2020). Natural convection in a partially heated porous cavity to Casson fluid. International Communications in Heat and Mass Transfer, 114, 104555. https://doi.org/10.1016/j.icheatmasstransfer.2020.104555
26. Das, M., Mahanta, G., Shaw, S., and Parida, S. B. (2019). Unsteady MHD chemically reactive double-diffusive Casson fluid past a flat plate in porous medium with heat and mass transfer. Heat Transfer—Asian Research, 48(5), 1761-1777. https://doi.org/10.1002/htj.21456
27. Shruthy, M., and Mahanthesh, B. (2019). Rayleigh-Bénard convection in Casson and hybrid nanofluids: An analytical investigation. Journal of Nanofluids, 8(1), 222-229. https://doi.org/10.1166/jon.2019.1571
28. Gresho, P. M., and Sani, R. L. (1970). The effects of gravity modulation on the stability of a heated fluid layer. Journal of Fluid Mechanics, 40(4), 783-806. https://doi.org/10.1017/S0022112070000447
29. Malashetty, M. S., and Padmavathi, V. (1997). Effect of gravity modulation on the onset of convection in a fluid and porous layer. International journal of engineering science, 35(9), 829-840. https://doi.org/10.1016/S0020-7225(97)80002-X
30. Chen, W. Y., and Chen, C. F. (1999). Effect of gravity modulation on the stability of convection in a vertical slot. Journal of Fluid Mechanics, 395, 327-344. https://doi.org/10.1017/S0022112099006011
31. Vanishree, R. K., and Anjana, K. (2017). The Study of Effects of Gravity Modulation on Double Diffusive Convection in Oldroyd-B Liquids. Global Journal of Science Frontier Research.
32. Siddheshwar, P. G., Bhadauria, B. S., and Srivastava, A. (2012). An analytical study of nonlinear double-diffusive convection in a porous medium under temperature/gravity modulation. Transport in porous media, 91, 585-604. https://doi.org/10.1007/s11242-011-9861-3
33. Bhadauria, B. S., and Kiran, P. (2015). Weak nonlinear double diffusive magneto-convection in a Newtonian liquid under gravity modulation. Journal of Applied Fluid Mechanics, 8(4), 735-746. https://doi.org/10.18869/acadpub.jafm.67.223.22740
34. Kiran, P. (2022). Gravitational modulation effect on double-diffusive oscillatory convection in a viscoelastic fluid layer. Journal of Nanofluids, 11(2), 263-275. https://doi.org/10.1166/jon.2022.1827
35. Kiran, P. (2023). Gravity modulation effect on weakly nonlinear thermal convection in a fluid layer bounded by rigid boundaries. International Journal of Nonlinear Sciences and Numerical Simulation, 24(3), 867-881. https://doi.org/10.1515/ijnsns-2021-0054
36. Akhila, P. A., Patil Mallikarjun B., and Kiran, P. (2023). Nonlinear double diffusive convection in bi-viscous Bingham fluid layer under gravity modulation. Authorea Preprints. https://doi.org/10.22541/au.169045968.85667456/v1

[1] Department of Studies and Research in Mathematics, Tumkur University, Tumakuru-572103, India.
Email address: chandankggs@gmail.com

[2] Department of Studies and Research in Mathematics, Tumkur University, Tumakuru-572103, India.
Email address: mbp1007@yahoo.com

[3] Department of Studies and Research in Mathematics, Tumkur University, Tumakuru-572103, India.
Email address: pa.akhila.1993@gmail.com